Radio-frequency dielectric measurements at temperatures from 10 to 450 K

R. Böhmer, M. Maglione,[a] P. Lunkenheimer, and A. Loidl
Institut für Physik, Universität Mainz, D-6500 Mainz, West Germany

(Received 21 July 1988; accepted for publication 5 October 1988)

A coaxial air line was constructed to connect a radio-frequency impedance analyzer and a temperature-stabilized sample holder. It is suitable for dielectric measurements in the frequency range 1 MHz–1 GHz and at temperatures between 10 and 450 K. The dielectric dispersion of Fe-doped $BaTiO_3$ and Na-doped KCN is presented. The results demonstrate the capability of this setup when investigating materials with high as well as with low dielectric constants.

I. INTRODUCTION

Dielectric measurements can provide important insights into the dynamics of molecular and ionic matter. For the complete characterization of the relaxational and resonant motional mechanisms involved, a large temperature range and a broad spectral frequency range are required. For the study of orientational polarization effects, i.e., for frequencies below some 10 GHz, automated measuring equipment is now commercially available. In the low-frequency range 0.1 mHz $< f <$ 1 MHz, where test-device dimensions are much smaller compared to the wavelength of the electric field, techniques using frequency response analysis are usually applied.[1] At higher frequencies resonance methods[2] and reflectometric methods[3–5] must be used. While the application of the first method is restricted to a finite number of frequencies, this is not true for the latter techniques.

For temperature-dependent measurements the test port of the radio-frequency analyzer and the sample holder must be thermally decoupled using a coaxial line. Therefore, an air line was constructed that is suitable for measurements from cryogenic temperatures up to $T = 450$ K. Construction and correct calibrations are described in the following section. Also included is a brief description of the experimental setup. Finally, results on some typical dielectrics are presented.

We are aware that similar experimental techniques have already been used elsewhere.[6] However, so far no detailed description of a setup for reflectivity measurements in the frequency domain covering the MHz–GHz range has come to our attention.

II. EXPERIMENT

A. Coaxial line

Coaxial semirigid cables, which provide a suitable connection between the measuring port and the temperature-controlled sample holder, may be obtained from several companies.[7] These exceedingly expensive cables consist of a dielectric material such as Teflon for low-temperature or magnesium oxide for high-temperature applications stabilizing two conducting tubes in concentric positions. For carrying out precise dielectric measurements in a wide temperature range, this causes a number of disadvantages: On the one hand, two different types of cables are necessary; on the other hand, the thermal changes of properties of the dielectric inside the line must be compensated for at a number of temperatures. To overcome these difficulties, an air line was constructed that is suitable for cryogenic and elevated temperatures. Because of the special construction, the calibration performed at room temperature was valid over the whole temperature range.

A drawing of the air line is shown in Fig. 1. It connects the network analyzer to a HP16091 sample holder[8] using commercial PC7 connectors (5).[7] Below the upper connector, a copper block (11) flanged to the cold head of the closed-cycle refrigerator guaranteed rapid thermalization when used at cryogenic temperatures. The sample (13) is inserted between two pins (3) at the end of the line. The upper pin was glued to the short (4) to facilitate sample changes. For low-temperature applications, in addition to the stainless-steel outer sleeve (7),[8] another sleeve (made of alumina) was used to reduce the thermal mass and thus to increase the cooling rate. A diode sensor on the lower end of the sleeve measured the sample temperature. For elevated temperatures a heater wire and a platinum sensor were immersed into a copper sleeve. The measuring signal was guided between two gold-plated stainless-steel tubes (9), whose

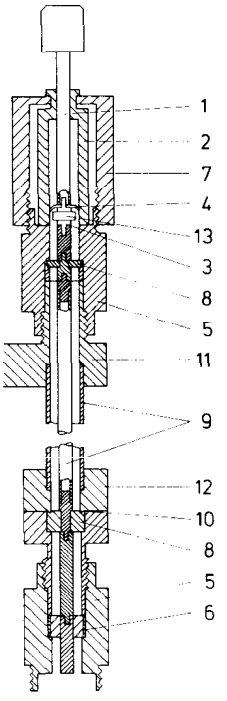

FIG. 1. Schematic drawing of the air line: Parts (1)–(6) are commercially available (Refs. 7 and 8): (1) ratchet, (2) ground sleeve, (3) pin, (4) spring from which the nonmetallic part was removed (for convenience the upper pin was attached with glue to the spring), (5) PC7 connector, (6) dielectric support ring, (7) sleeve, (8) Teflon ring (8.1-mm o.d. and 2.5-mm i.d.), (9) stainless-steel tubes (8-mm o.d. $\times$ 0.5-mm wall and 3-mm o.d. $\times$ 0.2-mm wall), (10) sealing edge, (11) copper block flanged to the cold head, (12) brass vacuum feedthrough, and (13) sample. All self-fabricated parts subjected to the electric field are plated with gold. The length from connector to connector is some 35 cm.

[a] Permanent address: Universite de Bourgogne, Laboratoire de Physique du Solide, B. P. 138, 21004 Dijon Cedex, France.

 0021-8979/89/030901-04$02.40

radii were chosen to match the characteristic impedance Z_0 of the network analyzer (here $Z_0 = 50\ \Omega$). Dielectric rings (6) and (8) center the inner tube. The upper one was made out of Teflon and was 1 mm thick. It was chosen to match the characteristic impedance (for the precise dimensions see the caption of Fig. 1). This minimum consumption of dielectric material exposed to other than room temperature leads to no measurable changes of the line characteristics from 10 to 450 K. However, probably due to intrinsic dispersion effects caused by the upper Teflon ring (8) dielectric losses centered around 250 MHz showed up at higher temperatures. These effects are negligible in investigations of materials with high dielectric constants, but they have to be taken into account when measuring insulators with low dielectric constants. To improve the performance of the line above 450 K the Teflon ring must be substituted by ceramic materials. Even at these elevated temperatures the influence of the thermal expansion of the stainless-steel tubes is negligible.

It was necessary to seal the inner and the outer tubes to achieve the vacuum required in cryogenics. Sealing of the outer tube is easily maintained with an O ring around the feedthrough (12). The inner tube, where the electric field traveled, was sealed with a 5-mm-long Teflon ring. The fringing effects caused by the special shape of the sealing edge (10) lead to no multiple reflections. This was concluded from the applicability of the calibration procedure given below, which was proven with the help of numerous standard impedances and samples.

The line shown in Fig. 1 is well characterized in the scheme of network theory[9] as a terminated two-port network (Fig. 2). The complex ratio of incident and reflected signals (the reflection coefficient Γ_S of the sample) is different from the measured reflection coefficient Γ. Γ is affected mainly by the absorption and phase shift inside the line and can be described by the S parameters of the network. Simplification rules for networks as shown in Fig. 2 lead to[9]

$$\Gamma_S = 1/[S_{00}/(\Gamma - S_{11}) + S_{22}] \tag{1}$$

with $S_{00} = S_{12}S_{21}$. To determine the frequency-dependent S parameters S_{00}, S_{11}, and S_{22}, the network is terminated with three different impedances. 0 Ω, 50 Ω, and 0 Ω^{-1} are standard, with reflection coefficients of $\Gamma_S = -1$, 0, and A, respectively; in the following, the constant A is assumed to be unity. However, radiation and fringe fields at the end of the coaxial line produce small deviations from unity as discussed in Ref. 3. The measured reflection coefficients are then Γ_{-1}, Γ_0, and Γ_1. Inserting these coefficients into Eq. (1) yields

$$S_{11} = \Gamma_0, \tag{2}$$

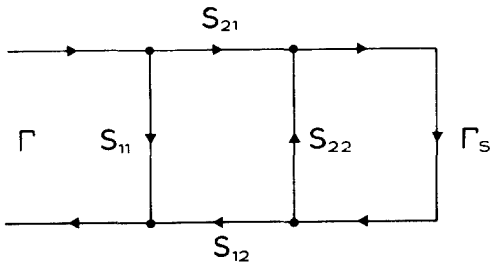

FIG. 2. Terminated two-port network with the S parameters defined in the conventional manner.

$$S_{22} = (\Gamma_1 + \Gamma_{-1} - 2\Gamma_0)/(\Gamma_1 - \Gamma_{-1}), \tag{3}$$

$$S_{00} = (\Gamma_0 - \Gamma_1)(1 + S_{22}). \tag{4}$$

The complex dielectric constant $\epsilon = \epsilon' - i\epsilon''$ is related to the reflection coefficient Γ_S by

$$\epsilon = (1 - \Gamma_S)/[(1 + \Gamma_S)i2\pi f C_0 Z_0], \tag{5}$$

where Z_0 is the characteristic impedance of the network analyzer and f is the measuring frequency. The dimensions of the sample determine $C_0 = \epsilon_0\, a/d$. ϵ_0 is the permittivity of free space, a is the area, and d is the thickness of the sample. The errors in ϵ introduced by the uncertainty of the sample dimensions are of the order of 1%. The error in Γ, which is given by the accuracy of the radio-frequency analyzer,[8] is not significantly increased when using the air line. For capacitances of the order of some 10 pF (which are the room-temperature values of our $BaTiO_3$ samples) the error due to the impedance analyzer (and thus the error in ϵ) never exceeds 5% over the entire frequency range.[8]

B. Temperature-controlled measurements

The measuring system used for cryogenic experiments is shown schematically in Fig. 3. Two sample temperature sensors, i.e., a Si diode for low temperatures and a Pt resistor for high temperatures, and the heater wire are attached to the sleeve at the end of the air line, as described above. Another sensor and heater connecting the cold stage of the refrigerator and the copper flange of the air line were used for low-temperature control. To reach 10 K, a radiation shield made of insulation foil wound on a copper tube (not shown in Fig. 3) had to be inserted between the sample and outer vacuum shield. The connection between the cold stage and copper flange was interrupted if elevated temperatures were required. All sensors and heaters are connected to a controller which itself is interfaced to a personal computer (PC).

The heater power for stabilizing a sample temperature of 450 K did not exceed 10 W, demonstrating the effective thermal decoupling achieved with the thin-walled stainless-steel tubes of the air line. Temperature stabilization was always better then 0.1 K.

Reflection coefficient data are transmitted from the network analyzer to the PC. The data are corrected for the

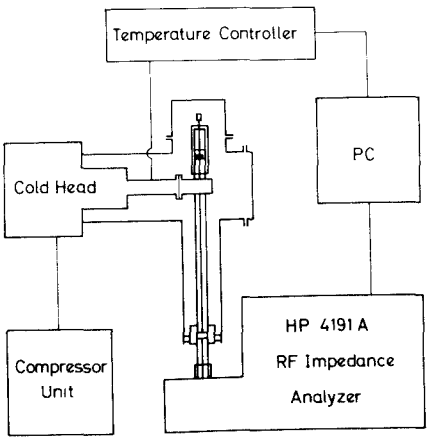

FIG. 3. Schematic drawing of the setup used for cryogenic measurements.

line effects and transformed to the complex dielectric constant. Further software processing includes graphic and fitting capabilities.

III. EXAMPLES OF MEASUREMENTS AND DISCUSSION

Different dielectric specimens were chosen to demonstrate the range of applications of the air line. First, measurements are presented on a material with a high dielectric constant, Fe-doped $BaTiO_3$. Then, results on Na-doped KCN crystals are shown to illustrate the capabilities of our setup when investigating low dielectric loss samples. When special attention is paid to contact resistances, this measuring system is also suitable for conducting materials.[10]

A. $BaTiO_3$:Fe

A good deal of the ionic motion in perovskitelike crystals is expected to be observable in the radio-frequency range.[11,12] $BaTiO_3$, as an example, is an extensively studied ferroelectric compound.[13] Fe-doped $BaTiO_3$ is suitable for a number of optical applications, e.g., holographic storage and phase conjugation.[13] The dynamics of the Ti^{4+} ion placed in an octahedral oxygen cage successively triggers three different ferroelectric transitions. A nonpolar cubic structure is stable at high temperatures. With decreasing temperatures $BaTiO_3$ transforms into phases with tetragonal, orthorhombic, and rhombohedral lattice distortions. These are characterized by spontaneous polarizations along the [100], [110], and [111] axes, respectively.

Figure 4 shows the real part of the dielectric constant ϵ' of $BaTiO_3$ (doped with 0.075% Fe). The sample was annealed at 480 K for several hours and cooled down to 10 K with a constant rate of 0.3 K per min. The three ferroelectric phase transitions are clearly established at 408.5, 280.2, and 181.0 K. The low-temperature data are in good agreement with results that were measured with a semirigid cable in a He-bath cryostat.[14]

We performed a systematic investigation of the dipolar dynamics in pure and doped $BaTiO_3$ single crystals at the cubic to tetragonal phase transition. A summary of the results will be given elsewhere.[15] As an example, Fig. 5 shows the dielectric constant of a 0.9%-Fe-doped $BaTiO_3$ sample. The results are presented using a Cole–Cole plot, where the imaginary part of the dielectric constant ϵ'' is plotted versus

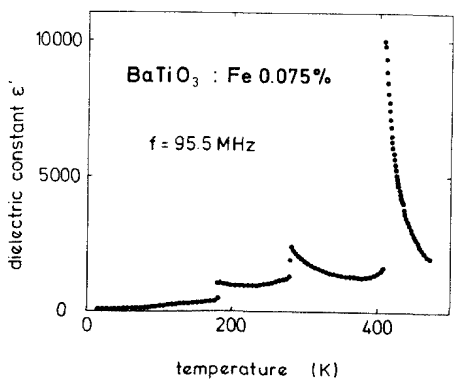

FIG. 4. Dielectric constant of $BaTiO_3$ doped with 0.075% Fe vs temperature for a measuring frequency of 95.5 MHz. The ferroelectric phase transitions appear as steps in the dielectric constant.

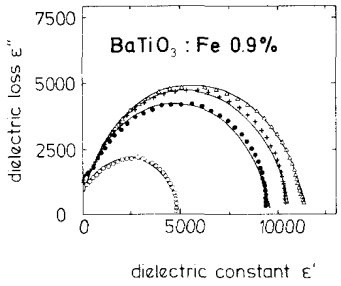

FIG. 5. Cole–Cole plot for $BaTiO_3$ doped with 0.9% Fe for different temperatures (391.6 K, ○; 393.3 K, ●; 395.4 K, +; 410.3 K, △). The solid lines are calculated using a Debye model.

the real part ϵ' for different temperatures above the ferroelectric phase transition. At all temperatures the results can be described by ideal Debye-type relaxations. The solid lines in Fig. 5 show the good agreement of fits with the experimental results.

B. KCN:Na

The alkali cyanide–alkali halide mixed crystals are model systems for orientational glasses. These systems provide good examples of low loss dielectric materials. The magnitude of the dielectric constant is typical for glasses and many nonpolar insulators. The mixed cyanide crystals exhibit extremely broad dielectric loss curves.[16] Hence, a large frequency range is experimentally required to determine the distribution of relaxation times and to follow the dipolar freezing-in over a wide temperature range. A dielectric investigation of KCN:Na mixtures at low frequencies has been published earlier.[16] Here we present some dielectric results as obtained at radio frequencies. Figure 6 shows the temperature dependence of the real part of the dielectric constant near the freezing temperature. For comparison, low-frequency results have also been included. For a detailed study of the freezing dynamics in orientational glasses it is essential to probe a wide frequency range.[17]

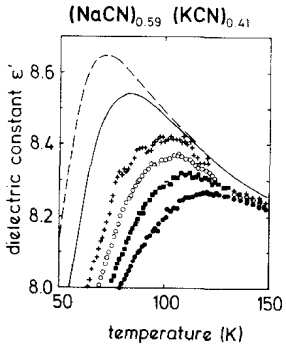

FIG. 6. Real part of the dielectric constant in $(NaCN)_{0.59}(KCN)_{0.41}$ vs temperature for different measuring frequencies (18.3 MHz, +; 41.7 MHz, ○; 144.5 MHz, □; 501.2 MHz, ●). The solid and the dashed lines represent the results of measurements at low frequencies (Ref. 16) (1 kHz, dashed line; 100 kHz, solid line).

IV. SUMMARY

An air line was described that is suitable for impedance measurements in a temperature range from 10 to 450 K and for frequencies between 1 MHz and 1 GHz. Formulas were given to calculate the complex dielectric constants of the samples from the measuring quantities. Measurements on samples with high and low dielectric constants have demonstrated the capabilities of this setup. Work is in progress to modify the air line for carrying out measurements at temperatures considerably higher than $T = 450$ K.

ACKNOWLEDGMENTS

This work was partly supported by the Deutsche Forschungsgemeinschaft within the Sonderforschungsbereich 262. The Fe-doped $BaTiO_3$ single crystals were kindly provided by G. Godefroy. We are indebted to U. T. Höchli for focusing our interest on high-frequency dielectric measurements and for many stimulating discussions. Useful conversations with F. Hufnagel and F. Kremer are acknowledged. We also thank our technical experts F. Kenntner and E. Griess.

[1]C. T. Morse, J. Phys. E 7, 657 (1974).
[2]For example, P. P. M. Groenewegen and R. H. Cole, J. Chem. Phys. **46**, 1069 (1967); M. D. Benadda, J. C. Carru, and C. Druon, J. Phys. E **15**, 132 (1982); A. Kakimoto, A. Etoh, K. Hirano, and S. Nonaka, Rev. Sci. Instrum. **58**, 269 (1987).
[3]T. Ichino, H. Ohkawara, and N. Sugihara, Hewlett-Packard J. **31**, 22 (1980).
[4]B. Haraoubia, J. L. Meury, and A. LeTraon, J. Phys. E **21**, 456 (1988).
[5]U. Kaatze and K. G. Giese, J. Phys. E **13**, 133 (1980).
[6]See, e.g., K. Deguchi, E. Nakamura, and K. Hirano, Ferroelectrics **67**, 23 (1986); J. C. Badot, A. Fourrier-Lamer, N. Baffier, and Ph. Colomban, J. Phys. (Paris) **48**, 1325 (1987).
[7]Huber & Suhner AG, Herisau, Switzerland, or Uniform Tubes, Inc., Collegeville, PA.
[8]Manual for the rf impedance analyzer 4191A including the operation note for the test fixture 16091A, Yokogawa–Hewlett-Packard, Tokyo, 1980.
[9]S. F. Adams, *Microwave Theory and Applications* (Prentice-Hall, Englewood Cliffs, NJ, 1969).
[10]M. Maglione, R. Böhmer, P. Lunkenheimer, M. Lotze, A. Loidl, and S. Kemmler-Sack, Physica C **153–155**, 649 (1988).
[11]M. Maglione, S. Rod, and U. T. Höchli, Europhys. Lett. **4**, 631 (1987), and references therein.
[12]K. A. Müller and W. Berlinger, Phys. Rev. B **34**, 6130 (1986).
[13]M. E. Lines and A. M. Glass, *Principles and Applications of Ferroelectrics and Related Materials* (Clarendon, Oxford, 1977).
[14]M. Maglione, E. Grymaszewski, and G. Godefroy (unpublished).
[15]M. Maglione, R. Böhmer, A. Loidl, and G. Godefroy, results presented at the International Conference on Defects in Insulating Crystals, Parma, 1988 (unpublished).
[16]A. Loidl, T. Schräder, R. Böhmer, K. Knorr, J. K. Kjems, and R. Born, Phys. Rev. B **34**, 1238 (1986).
[17]U. G. Volkmann, R. Böhmer, A. Loidl, K. Knorr, U. T. Höchli, and S. Haussühl, Phys. Rev. Lett. **56**, 1716 (1986).